HHS Public Access

Author manuscript

Nat Commun. Author manuscript; available in PMC 2015 January 08.

Published in final edited form as:

Nat Commun. ; 5: 4259. doi:10.1038/ncomms5259.

IL-23 Promotes TCR-mediated Negative Selection of Thymocytes through the Upregulation of IL-23 Receptor and RORγt

Hao Li[1,2], **Hui-Chen Hsu**[1], **Qi Wu**[1], **PingAr Yang**[1], **Jun Li**[1], **Bao Luo**[1], **Mohamed Oukka**[3], **Claude H. Steele III**[4], **Daniel J Cua**[5], **William E. Grizzle**[6], and **John D. Mountz**[1,7]

[1]Division of Clinical Immunology & Rheumatology, Department of Medicine, University of Alabama at Birmingham

[2]Dept. Microbiology, University of Alabama at Birmingham

[3]Department of Pediatrics, University of Washington, Seattle, WA

[4]Division of Pulmonary, Allergy & Critical Care, Dept. Medicine, University of Alabama at Birmingham

[5]Merck Research Laboratories, Palo Alto, CA

[6]Clinical Pathology & Anatomic Pathology, University of Alabama at Birmingham

[7]Birmingham VA Medical Center

Summary

Transient thymic involution is frequently found during inflammation, yet the mode of action of inflammatory cytokines is not well defined. Here we report that interleukin-23 (IL-23) production by the thymic dendritic cells (DCs) promotes apoptosis of the $CD4^{hi}CD8^{hi}$ double positive (DP) thymocytes. A deficiency in IL-23 signaling interferes with negative selection in the male D^b/H-Y T-cell receptor (TCR) transgenic mice. IL-23 plus TCR signaling results in significant up-regulation of IL-23 receptor (IL-23R) expressed predominantly on $CD4^{hi}CD8^{hi}CD3^{+}\alpha\beta TCR^{+}$ DP thymocytes, and leads to RORγt dependent apoptosis. These results extend the action of IL-23 beyond its peripheral effects to a unique role in TCR mediated negative selection including elimination of natural T regulatory cells in the thymus.

Corresponding authors: Hui-Chen Hsu, Ph.D and John D. Mountz, M.D., Ph.D SHEL 307, 1825 University Blvd, Birmingham, AL 35294; Phone: 205-934-8909, rheu078@uab.edu (H.-C.H.) and jdmountz@uab.edu (J.D.M.).

Competing financial interests: The authors declare no competing financial interests.

Author contributions

H.L., H.-C.H. and J.D.M. designed the research and wrote the manuscript. H.L., Q.W., P.A.Y., J.L., and B.L. conducted the experiments. M.O. provided IL-23R-GFP KI and the homozygous *Il23r*$^{-/-}$ mice and discussed the data; D.J.C. provided the *Il23 p19*$^{-/-}$ mice and discussed the data; C.H.S. III contributed to all experiments related with *Aspergillus fumigatus* infection; W.E.G. contributed to imaging data analysis and interpretation.

Introduction

The thymic environment orchestrates the development of the diverse repertoire of functional T cells that is required for a robust adaptive immune response to foreign antigens (Ags) while minimizing the generation of T lymphocytes that can attack normal tissues and drive autoimmunity[1]. One key control point in the thymus to maintain self-tolerance involves deletion of those late-stage $CD4^+CD8^+$ double positive (DP) thymocytes that express autoreactive αβTCRs and can interact with moderate to high affinity with thymic dendritic cells (DCs) presenting self-antigens [2–4]. Although other antigen-presenting cells in the thymus are involved in negative selection, the high levels of expression of major histocompatibility (MHC) and co-stimulatory molecules on the DCs make them essential for efficient negative selection[5–7].

The synchronized transitions of the gene expression profiles of the developing thymocytes are associated with alterations in the activity of critical transcription factors. One of these, the thymus-specific isoform of the retinoic acid receptor-related orphan receptor (RORγt) is normally only expressed at high levels in early-stage DN and DP thymocytes [8]. It promotes the development and survival of the early-stage DP thymocytes, following expression of the αβTCR, by activating transcription of the gene encoding the anti-apoptotic protein Bcl-xL [9,10] which then inhibits the transcription of *c-Rel* and *Il2* [8,11]. During the later stages of thymocyte development, down-regulation of RORγt is essential for the maturation of DP thymocytes into SP thymocytes because RORγt transgene expression in mature T cells affects their multiple functions including enhanced apoptosis and reduced proliferation [8,12,13]. It has been reported that ectopic over-expression of RORγt results in apoptosis instead of survival of DP in transition to SP thymocytes [14]. Thus, regulation of RORγt can be one factor deciding the fate of late stage DP thymocytes.

The signaling mechanisms that regulate RORγt expression in late stage DP thymocytes have not been identified. It has been shown that IL-23, a highly conserved member of the IL-12 family of regulatory cytokines that is primarily produced by DCs and macrophages [15,16], signals through RORγt in activated CD4 T cells in the periphery [17–19]. In the present study, we investigated whether IL-23 acts through the regulation of RORγt to regulate thymocyte selection. We have made an interesting observation that deficiency of the p19 subunit of IL-23 ($p19^{-/-}$) significantly reduced thymocyte apoptosis following *Aspergillus fumigatus* infection in B6 mice. It also perturbed thymic negative selection in male *Il23* $p19^{-/-}$ D^b/H-Y TCR transgenic (Tg) mice without affecting thymocyte positive selection in female *Il23* $p19^{-/-}$ D^b/H-Y TCR transgenic mice. Over-expression of IL-23 leads to enhanced apoptosis and depletion of late-stage DP thymocytes by up-regulation of RORγt and IL-23R via a TCR/CD3 dependent mechanism. The finding of IL-23-dependent negative selection may indicate a novel central regulation mechanism mediated by a cytokine that is proinflammatory in the periphery.

Results

IL-23 drives thymocyte apoptosis during infection

IL-23 is important in regulating clearance of pathogens[20–22], but also is associated with inflammation in autoimmune diseases, multiple sclerosis[23,24], rheumatoid arthritis[25], and lupus[26]. In an attempt to study the anti-fungal effect of IL-23 in clearance of *Aspergillus fumigatus*, we have made a surprising observation that despite the essential role of IL-23 in maintaining host resistance to this pathogen (Supplementary Fig. 1a), there was a substantial reduction in thymic size and total thymocyte count on day 4 in normal B6 mice (Supplementary Fig. 1b). TUNEL and 7-AAD staining indicated that the loss of thymocytes in wild-type (WT) B6 mice was associated with a dramatically increased apoptosis of $CD4^+CD8^+$ DP thymocytes (Supplementary Fig. 1c, 1d). FACS analysis showed a significant elimination of the $CD4^+CD8^+$ DP population (Supplementary Fig. 1e). In contrast, although a deficiency of IL-23 in B6-*Il23 p19*$^{-/-}$ mice enhanced *Aspergillus fumigatus*-induced mortality, the massive loss of thymic cellularity and DP thymocytes were largely circumvented (Supplementary Fig. 1a–1e). Interestingly, IL-23 receptor (IL-23R), which was detected in a small percent of DP thymocytes of naïve mice, was significantly upregulated on day 3 in DP thymocytes of *Aspergillus fumigatus*-infected WT but not B6-*Il23 p19*$^{-/-}$ mice (Supplementary Fig. 1f). During the course of infection, IL-23 levels were dramatically elevated between days 1 to 2 (Supplementary Fig. 1g). These above findings suggest an interesting concept that IL-23 may potentially affect thymic output.

Decreased thymic negative selection in *Il23 p19*$^{-/-}$ mice

To determine if IL-23 play a role in thymic selection, we crossed *Il23 p19*$^{-/-}$ to D^b/H-Y TCR Tg background and examined thymocyte negative or positive selection in the male versus female mice, respectively [27–29], to determine if IL-23 directly plays a role in regulating thymocyte development. In the male mice, the cortical area of the thymus of the *Il23 p19*$^{-/-}$ D^b/H-Y TCR mice was enlarged compared to the *Il23 p19*$^{+/+}$ D^b/H-Y TCR mice (Fig. 1a). The thymi were not overtly different in the female *Il23 p19*$^{-/-}$ D^b/H-Y TCR Tg mice compared to the female *Il23 p19*$^{+/+}$ D^b/H-Y TCR Tg mice (Fig. 1b).

There were a higher percentage and increased cell counts of both DP and $CD8^+$ SP thymocytes in the *Il23 p19*$^{-/-}$ D^b/H-Y -TCR Tg male mice as compared to the *Il23 p19*$^{+/+}$ D^b/H-Y-TCR Tg male mice, which is consistent with a defect in thymic negative selection (Fig. 1c, 1d, 1e). The lack of significant differences in the sizes of the thymocyte subpopulations in the female *Il23 p19*$^{+/+}$ D^b/H-Y TCR Tg mice and female *Il23 p19*$^{-/-}$ D^b/H-Y- TCR Tg mice further suggests that IL-23 is not involved in thymic positive selection (Fig. 1f, 1g, 1h). The thymic negative selection is a highly specialized process for DP thymocytes that takes place in the thymic medullary areas where tissue-restricted antigens in the periphery are presented. Consistently, the majority of $TUNEL^+$ cells were detected in the inner cortex and the medullary area near the vicinity of the thymic $S100^+$ DCs in *Il23 p19*$^{+/+}$ D^b/H-Y TCR Tg thymus (Fig. 1i). The numbers of the apoptotic cells were dramatically lower in the *Il23 p19*$^{-/-}$ D^b/H-Y TCR Tg male mice (Fig. 1i) and the frequency of apoptotic thymocytes was significantly lower especially in thymic medullary areas of the *Il23 p19*$^{-/-}$ D^b/H-Y TCR Tg male than in the *Il23 p19*$^{+/+}$ D^b/H-Y Tg male

mice (Fig. 1j). There was a significantly higher expression of IL-23 receptor (IL-23R) on DP thymocytes in *Il23 p19*$^{+/+}$ D^{b}/H-Y TCR Tg male mice comparing to *Il23 p19*$^{-/-}$ D^{b}/H-Y TCR Tg male mice (Supplementary Fig. 2a). Interestingly, the IL-23R expression on DN thymocytes from both strains are not detectable even those cells have early expression of transgenic TCR (Supplementary Fig. 2a). Together, these results suggested that there is tight temporal and spatial regulation of IL-23 mediated thymic selection.

Decreased thymocyte apoptosis in naïve B6-*Il23 p19*$^{-/-}$ mice

To further verify our findings, we determined the tissue related expression of *Il23 p19* and *Il23r* in naïve C57BL/6 mice. The results showed that, compared to spleen, lymph nodes (LN), kidney, liver, and colon, thymus expresses higher levels of both *Il23* and *Il23r* (Supplementary Fig. 2b). Within different populations of cells sorted from the thymus of naïve B6 mice using the protocol shown in Supplementary Fig. 3[30,31], thymic DCs expressed dramatically higher levels of *Il23*, compared to cortical epithelial cells (cTECs) and medullary thymic epithelial cells (mTECs) (Fig. 2a). Furthermore, *Il23r*, but not *Il23*, mRNA was detectable in Thy1.2^{+} thymocytes (Fig. 2b). Within subpopulations of thymocytes, the levels of *Il23r* were the highest in CD4^{hi}CD8^{hi} DP thymocytes and were almost undetectable in DN and CD8 SP cells (Fig. 2b). *Il23r* was also detected in thymic epithelial cells and DCs (Fig. 2b).

The specificity of a polyclonal anti-IL-23R antibody was confirmed by analysis on i*n vitro* polarized Th17 and Th1 cells generated from heterozygous IL-23R-green fluorescent protein (GFP) knock-in mouse spleen [32,33] (Supplementary Fig. 4). Using this anti-IL-23R antibody, we have identified that IL-23R was expressed by a small percent of thymocytes and the majority of these cells were within the CD4^{+}CD8^{+} DP thymocyte population (Fig. 2c). The IL-23R^{+} population was almost undetectable in IL-23R deficient mice (Fig. 2c). Interestingly, the percent of this small population of IL-23R^{+}CD4^{hi}CD8^{hi} DP thymocytes gradually decreases with increasing age, suggesting the close association with the rate of thymopoiesis (Fig. 2d and Supplementary Fig. 5).

We next determined if a deficiency of *Il23* was associated with decreased apoptosis. *In situ* TUNEL staining revealed that the numbers of thymocytes undergoing apoptosis were reduced in *Il23 p19*$^{-/-}$ mice compared to wild-type B6 mice (Fig. 2e), and the reduction was apparent especially in the inner cortex and cortical-medullary (CM) junction (Fig. 2f). The location of TUNEL^{+} thymocytes was determined along with co-staining for S100^{+} thymic DCs. In WT B6 mice, TUNEL^{+} thymocytes were predominately found in close proximity to the S100^{+} thymic DCs. In contrast, in *Il23 p19*$^{-/-}$ B6 mice, there were fewer TUNEL^{+} apoptotic thymocytes (Fig. 2g). These results are consistent with findings derived from *Aspergillus fumigatus*-infected mice or D^{b}/H-Y TCR Tg male mice to suggest that the major function of IL-23R signaling in the thymus is to induce thymocyte apoptosis.

Delayed apoptosis induced by IL-23 in the thymus

To enable us to follow the kinetics of IL-23-mediated thymocyte apoptosis, exogenous IL-23 was induced by administration of an adenovirus that carries the mouse *Il23* gene (AdIL-23) to naïve B6 mice [34,35]. An adenovirus carrying the *LacZ* gene (AdLacZ) was

used as a control. The serum levels of IL-23 in the AdIL-23-injected mice were increased over baseline by day 3, reached the maximal value at day 5, were maintained until day 9 and returned to baseline by day 10 (Supplementary Fig. 6a). The size of the thymus and its cellularity began to diminish in the AdIL-23-injected mice on day 7 (2 days after the peak level of IL-23 in the sera) (Fig 3a and Supplementary Fig. 6b). Consistent with this, the most significant depletion of the DP thymocytes occurred on day 9 (Supplementary Fig. 6b). Flow cytometry analysis revealed that the earliest depletion could be observed in the $CD4^{hi}CD8^{hi}$ population 5 days after administration of the AdIL-23 whereas the $CD4^{lo}CD8^{lo}$ population became involved somewhat later (by day 7), with the greatest decrease seen at day 9 (Fig. 3b and Supplementary Table 1). Histological staining confirmed a delayed loss of the thymic cortex after AdIL-23 administration (Fig. 3c and Supplementary Table 2). This loss correlated with a dramatically higher level of apoptosis and lower proliferation of thymocytes (Fig. 3d, 3e, and Supplementary Table 2). zVAD, a pan-caspase inhibitor, *in vivo* treatment significantly blocked the IL-23 mediated thymic cellularity loss, which suggests that IL-23 primarily acts through induction of apoptosis to diminish thymus size and thymocyte count in mice (Supplementary Fig. 7). Interestingly, the delayed peak of apoptosis after AdIL-23 does not correlate with the early phase of cytokine induction, and is not observed in control AdLacZ administered mice.

IL-23R is required for IL-23-induced thymocyte apoptosis

Based on the finding in *Aspergillus fumigatus*-infected mice that IL-23R upregulation was associated with the massive thymocyte apoptosis, we determined if the delayed onset of exogenous AdIL-23 induced thymocyte apoptosis is related to the requirement of IL-23R upregulation. AdIL-23 or AdLacZ was administered to mice that lack the IL-23R (homozygous IL-23R-green fluorescent protein knock-in mice) [36]. Neither the reduction in thymus size nor the depletion of DP thymocytes that was observed in AdIL-23-treated wild-type $Il23r^{+/+}$ mice was apparent in the AdIL-23-treated $Il23r^{-/-}$ mice (Fig. 4a, 4b, Supplementary Table 3).

To confirm that IL-23R expression on thymocytes, but not other thymic cells including TEC or DCs that also expressed IL-23R, was essential for IL-23 induced apoptosis, bone marrow (BM) reconstitution was carried out in 3 conditions (WT → WT, WT → $Il23r^{-/-}$ and $Il23r^{-/-}$ → WT). In this experimental condition, DCs and macrophages are more susceptible to radiation induced apoptosis compared to the epithelial cells ($CD45^{-}$) [37,38] and thymocytes do not repopulate normally without TECs [39]. We have identified that in all 3 groups of chimeric mice, there was nearly complete reconstitution of thymocytes, and almost all were derived from transferred donor BM at Day 40 (Supplementary Fig. 8a, 8b). The thymic $CD11b^{+}$ or $CD11c^{+}$ cells, however, remained as recipient origin (Supplementary Fig. 8c), suggesting that recipient DCs and TECs remained unaffected under the present experimental condition.

AdIL-23 or control AdLacZ was then administered to these three groups of mice. A specific requirement for IL-23R expression on thymocytes to drive apoptosis induced by AdIL-23 is indicated by the dramatically decrease in the sizes of the thymi in both WT → WT and in WT → $Il23r^{-/-}$ mice compared to $Il23r^{-/-}$ → WT on day 9 after AdIL-23 administration

(Fig. 4c and Supplementary Fig. 8d, 8e). A significantly loss of the thymic cortex and a higher level of apoptosis were shown in the thymi of AdIL-23 administered recipients from both WT → WT and WT → *Il23r*$^{-/-}$ groups compared to *Il23r*$^{-/-}$ → WT group by histology staining (Fig. 4d, 4e). Depletion of the DP thymocytes was also seen in the thymi of AdIL-23 administered WT → WT and WT → *Il23r*$^{-/-}$ groups but was less apparent in those from the *Il23r*$^{-/-}$ → WT group (Fig. 4f). As only thymocytes derived from *Il23r*$^{+/+}$ donor cells exhibited high sensitive to AdIL-23-mediated thymocyte depletion, these results suggest that IL-23R expressed on thymocytes rather than non-thymocytes plays a key role for IL-23 induced thymocyte apoptosis. Consistent with these results, we have identified that AdIL-23 depleted *Il23r*$^{+/+}$ thymocytes but spared *Il23r*$^{-/-}$ thymocytes in recipient mice that have been reconstituted with a 50: 50 ratio of mixed bone marrow from congenically marked CD45.1 *Il23r*$^{+/+}$ + CD45.2 *Il23r*$^{-/-}$ mice (Supplementary Fig. 9), suggesting the high death rate of IL-23R^{+} thymoyctes when encountering IL-23.

IL-23 upregulates IL-23R to amplify IL-23-induced apoptosis

In peripheral T cells, the expression of IL-23R is induced by their activation and further enhanced by IL-23 [17,18]. Our data showed that only a minor population of DP thymocytes expressed IL-23R under naïve conditions (Supplementary Fig. 1f and Fig. 2c, 2d). To determine if AdIL23 administration could upregulate IL-23R expression prior to induction of apoptosis, we examined IL-23R expression within the thymus *in vivo* at different time points after administration of either AdIL-23 or AdLacZ. The majority of IL-23R^{+} thymocytes were confined to the CD4^{hi}CD8^{hi} DP subset and the frequency of these IL-23R^{+}CD4^{hi}CD8^{hi} DP thymocytes was significantly higher in the AdIL-23-treated mice than in the AdLacZ-treated mice especially on day 5 (Fig. 5a). Immunofluorescence confocal microscopy analysis showed a dramatic increase of IL-23R^{+} thymocytes in the cortical medulla junction areas of thymus 5 days after AdIL-23 administration (Fig. 5b). Four days later, thymocytes that express IL-23R progressed to apoptosis as indicated by an increased population of IL-23R^{+} TUNEL^{+} thymocytes (Fig. 5b). We further utilized the heterozygous IL-23R-GFP KI mouse to determine expression of IL-23R *in vivo* by GFP fluorescence. Immunofluorescence confocal microscopy analysis indicated that the GFP^{+} cells colocalized with Thy1.2^{+} cells in the thymus of the AdIL-23-treated IL-23R-GFP KI mice 5 days after treatment (Fig. 5c, d, **right panels**). Few GFP^{+} cells can be detected in the thymi of AdLacZ-treated IL-23R-GFP KI mice (Fig. 5c, d, **left panels**). These results suggest that AdIL-23 upregulates IL-23R expression and further results in IL-23 mediated apoptosis which leads to the final loss of IL-23R^{+} subpopulation of thymocytes.

IL-23R-RORγt mediated CD4^{hi}CD8^{hi} DP thymocyte apoptosis

The roles of RORγt in thymocyte maturation and differentiation have been an interesting question as both RORγt deficient mice and RORγt transgene (Tg) mice have dramatically decreased cellularity in the thymus [8,10]. If IL-23-IL-23R primarily acts on late stage DP thymocyte apoptosis, this suggests that IL-23 may preferentially regulate the expression of RORγt in late versus early DP thymocytes. Comparison of the transcription levels of *Rorc* and *Il23r* in FACS-sorted CD4^{hi}CD8^{hi} DP thymocytes and CD4^{lo}CD8^{lo} DP thymocytes from either AdLacZ-treated or AdIL-23-treated mice 5 days after treatment revealed that the levels of *Rorc* and *Il23r* were similar in FACS-purified CD4^{lo}CD8^{lo} DP thymocytes from

mice administered with AdIL-23 or AdLacZ (Fig. 6a). In contrast, the FACS-purified $CD4^{hi}CD8^{hi}$ DP thymocytes from mice administered with AdIL-23 exhibited significantly higher levels of *Rorc* and *Il23r* than FACS-purified $CD4^{hi}CD8^{hi}$ DP thymocytes from AdLacZ-treated mice (Fig. 6a), suggesting that late-stage DP thymocytes are sensitive to AdIL-23-induced up-regulation of both Il23r and Rorc.

Complete absence of RORγt leads to survival defects of early DP thymocytes[10] and will not be informative to address the selective effects of RORγt in late stage DP thymocytes. To circumvent this, we utilized heterozygous $Rorc^{+/-}$ not $Rorc^{-/-}$ mice to determine if lower expression of *Rorc* could partially rescue $CD4^{hi}CD8^{hi}$ thymocytes from AdIL-23 mediated apoptosis (Fig. 6b). On day 9 after AdIL-23 or AdLacZ administration, the frequency of DP thymocytes was similar in the control AdLacZ-treated $Rorc^{+/-}$ and $Rorc^{+/+}$ mice. The frequency of DP thymocytes in the AdIL-23-treated mice $Rorc^{+/-}$ mice was comparable to that in the AdLacZ-treated $Rorc^{+/-}$ mice but was substantially higher than in the AdIL-23-treated $Rorc^{+/+}$ mice (Fig. 6b). The cell count confirmed that DP especially those $CD4^{hi}CD8^{hi}$ thymocytes from $Rorc^{+/-}$ mice are much less sensitive to IL-23 induced apoptosis compared to $Rorc^{+/+}$ mice (Supplementary Table 3). Moreover, at day 5 post-AdIL-23 treatment, prior to the dramatic deletion of DP thymocytes, the induction of *Il23r* in the $CD4^{hi}CD8^{hi}$ DP thymocytes from $Rorc^{+/-}$ mice was substantially lower than that in $Rorc^{+/+}$ mice (Fig. 6c). These results suggest that IL-23-mediated induction of RORγt in late stage $CD4^{hi}CD8^{hi}$ DP thymocytes is associated with deletion, but not survival of thymocytes.

Target genes of *Rorc* in the thymus include *c-Rel* and *Bcl-xl* [8–10,14,40]. Analysis of the $CD4^{hi}CD8^{hi}$ DP subset indicated that AdIL-23 treatment was associated with a significant reduction in the levels of *c-Rel* but did not alter the expression of *Bcl-xl* in this subset in wild-type mice (Fig. 6d). The levels of both *c-Rel* and *Bcl-xl* in the $CD4^{lo}CD8^{lo}$ thymocytes were unaffected by AdIL-23 treatment. In contrast, partial deficiency of RORγt prevented AdIL-23 induced suppression of *c-Rel* in $CD4^{hi}CD8^{hi}$ but exhibited no effects of its expression in $CD4^{lo}CD8^{lo}$ thymocytes (Fig. 6d). Collectively, these results indicate that IL-23 acts through the IL-23R to up-regulate RORγt in the late-stage DP thymocytes. Down regulation of the levels of *c-Rel* is associated with IL-23-induced thymocyte apoptosis in $CD4^{hi}CD8^{hi}$ late stage DP but not $CD4^{lo}CD8^{lo}$ early stage DP thymocytes.

Antigen activation initiates the expression of IL-23R

Negative selection of thymocytes requires a strong TCR-self Ag interaction [29]. Consistent with the observation that IL-23-mediated thymocytes apoptosis was associated with negative selection, we observed that $IL\text{-}23R^{+}$ DP cells expressed higher levels of CD3 and αβTCR as indicated by gating on the $IL\text{-}23R^{+}$ population compared to the $IL\text{-}23R^{-}$ population (Fig. 7a). To determine if loss of TCR stimulation could prevent the up-regulation of IL-23R on thymocytes, we administered AdIL-23 to female D^{b}/H-Y TCR Tg mice in which the restricted T cell receptors were not responsive to all potential endogenous or exogenous antigens during the treatment. Reduction of both the size and cellularity of the thymi were not apparent in female D^{b}/H-Y TCR Tg mice but could be observed in wild type female B6 mice 9 days after AdIL-23 treatment (Fig. 7b). Histological staining confirmed a

significantly induction of apoptosis in thymic cortex of AdIL-23 treated female B6 mice but not D^b/H-Y TCR Tg mice (Fig. 7c, d). There was no increase of IL-23R$^+$ DP thymocytes in the thymi of AdIL-23 treated female D^b/H-Y TCR Tg mice compared with thymocytes from the B6 counterparts 9 days after AdIL-23 administration at which time the $CD4^{hi}CD8^{hi}$ population from the thymi of AdIL-23 treated female D^b/H-Y TCR Tg mice was almost not affected by IL-23 mediated apoptosis (Fig. 7e).

To further verify that TCR stimulation is necessary for IL-23-induced thymocyte apoptosis machinery, we co-cultured thymocytes from female D^b/H-Y TCR Tg mice with irradiated spleen cells from B6 female or male mice in the presence and absence of IL-23. Depletion of $CD4^+CD8^+$ thymocytes and expression levels of RORγt in the thymocytes cultured with irradiated female spleen stimulator cells did not differ with or without IL-23, presumably because the thymocytes lacked IL-23R induced by specific Ag stimulation (Fig. 7f). In contrast, co-culture of thymocytes from female D^b/H-Y TCR Tg mice with irradiated spleen cells from B6 male mice resulted in a significant upregulation of IL-23R, increased expression of RORγt and increased apoptosis. Furthermore, addition of IL-23 further upregulated both IL-23R and RORγt and greatly enhanced apoptosis (Fig. 7f). Similar results were observed after co-culture of MHC class-II restricted $MOG_{35–55}$ -reactive thymocytes from 2D2 TCR transgenic mice with MOG-pulsed irradiated spleen cells in the presence of IL-23 (Supplementary Fig. 10).

IL-23 preferentially eliminates nTreg thymocytes

One puzzle is the action of IL-23 mediated deletion of self-reactive T cells in the thymus seem to be in opposition to its well known pro-inflammatory role in the different autoimmune diseases [23,24,40]. We thus used Foxp3-GFP mice to track the percent of $Foxp3^+Helio^+$ natural occurring Treg (nTreg) cells after adenovirus administration. There was a significant reduction of nTregs in the thymus (Supplementary Fig. 11) in the AdIL-23 administered group, comparing to AdLacZ treated control group. Consistent with these findings, following AdIL-23 adminstration, in the spleens of WT CD45.1: *Il23r*$^{-/-}$ CD45.2 mixed BM reconstituted mice, the nTreg population was primarily *Il23r*$^{-/-}$ CD45.2 cells whereas the Th17s were primarily from *Il-23*$^{+/+}$ CD45.1 origin (Supplementary Fig. 12a–f). These data are consistent with recent studies that high levels of IL-23 was associated with increasing Th17s [40–42] and reduced Tregs [40,43]. IL-23 elimination of nTregs in the thymus may therefore act in concert with IL-23 in the periphery to promote autoimmune disease.

Discussion

Our present study advances the present understanding of IL-23 and negative selection in that it implicates IL-23 mediates apoptosis during the process of negative selection in the thymus. The current concept of negative selection is that the induction of apoptosis during negative selection is driven by direct cell contact between the self-antigen presenting cells and the thymocytes expressing self-reactive TCRs [44]. It has been shown that the process of negative selection is less stringent than positive selection because negative selection is never 100% complete and is always associated with some leakage of self-reactive T cells [45]. The present findings are consistent with this variability in that they indicate that while the cell-

cell interactions define the specificity of negative selection, IL-23 signaling can act as a second regulatory mechanism that defines the susceptibility of the interacting thymocytes to undergo apoptosis. The current studies do not rule out the possibility that, under some circumstances, higher affinity cell interactions may result in apoptosis in the absence of IL-23 or other cytokine signaling but do suggest that strong IL-23 signaling acts as adjuvant effects to down-regulate the threshold of TCR-mediated apoptosis and promotes the elimination of a great proportion of potentially self-reactive thymocytes.

The present results suggest that the IL-23-mediated thymocyte apoptosis is under both temporal and spatial regulation. The IL-23 specifically targets the $CD4^{hi}CD8^{hi}$ $CD3^{+}\alpha\beta TCR^{+}$ late-stage DP thymocyte subset in naïve mice and this highly specific targeting appears to be enforced through several mechanisms. IL-23R expression is limited to a small subset of thymocytes that are phenotypically identical to late-stage DP thymocytes. Within this population, its expression is induced by TCR engagement, suggesting that the interactions with the DCs are a triggering mechanism, and are subsequently enhanced by endogenous IL-23. Moreover, the downstream target of IL-23 signaling of apoptosis is RORγt, a thymus-specific isoform of RORγ, which is expressed predominantly in DP thymocytes [46]. RORγt activates the gene encoding the anti-apoptotic protein Bcl-xL and which has been shown to be required for the survival of early DP thymocytes [10]. Paradoxically, enforced expression of RORγt also lead to dramatic reduction of DP thymocytes [46]. The present findings unify these two apparently contradictory results and directly demonstrate that preferential expression of IL-23R in the late versus early DP thymocytes along with the migration of late DP thymocytes to the IL-23 producing thymic DC area in the medulla lead to differential RORγt mediated apoptosis versus survival. Furthermore, the IL-23/RORγt-mediated late DP thymocyte apoptosis does not affect the expression of *Bcl-xl* but is associated with a significant decline in *c-Rel*. Interestingly, a relatively small change in *Rorc* was found to exhibit remarkable impact on IL-23R-mediated thymocyte apoptosis. Such results underscore the importance in fine-tuning the expression of *Rorc* in regulating $IL\text{-}23^{+}TCR$ signaling-induced late stage DP thymocyte apoptosis.

Induction of thymocyte apoptosis by IL-23 overexpression required IL-23R expression, as apoptosis was not increased in treated $Il23r^{-/-}$ mice. Although IL-23R were expressed on different types of cells, the requirement for IL-23R expression on thymocytes but not non-thymocytes for the most efficient IL-23 induced apoptosis was shown by BM reconstitution of CD45.2 $Il23r^{-/-}$ mice with BM from CD45.1 WT mice. Furthermore, in IL-23R intact mice, 5 days after AdIL-23 administration, IL-23R was highly upregulated on $CD4^{hi}CD8^{hi}$ thymocytes, which correlates with the peak levels of IL-23 in the sera and the initial loss of $CD4^{hi}CD8^{hi}$ thymocytes. Although IL-23R is predominantly expressed on $CD4^{hi}CD8^{hi}$ thymocytes, on subsequent days, there was extensive reduction of both $CD4^{hi}CD8^{hi}$ and $CD4^{lo}CD8^{lo}$ thymocytes. We proposed that the loss of $CD4^{hi}CD8^{hi}$ thymocytes promoted the maturation of $CD4^{lo}CD8^{lo}$ thymocytes to $CD4^{hi}CD8^{hi}$ thymocytes which then undergo rapid apoptosis mediated by IL-23. This is supported by the observation that on day 9 after AdIL-23, IL-23R expression colocalized with TUNEL staining, indicating that $IL\text{-}23R^{+}$ thymocytes underwent apoptosis. Taken together, we conclude that IL-23 directly induces apoptosis of late-stage DP thymocytes subpopulation.

One unexpected finding is the complexity of IL-23 receptor induction and expression on thymocytes. Induction of IL-23R on $CD4^{hi}CD8^{hi}$ thymocytes requires antigen stimulation. IL-23R up-regulation and the following apoptosis progress were not observed in AdIL-23 treated D^b/HY TCR transgenic female mice due to the lack of H-Y male antigen stimulations. The requirement of TCR engagement for induction of IL-23R was further demonstrated *in vitro* by co-culture of thymocytes from MHC class I (D^b/H-Y, female) or class II (2D2) TCR transgenic mice with cells presenting D^b/H-Y or $H2^b/MOG_{35–55}$ antigen, respectively. However, analysis of IL-23R on DN thymocytes in D^b/H-Y TCR Tg male mice shows that despite the early assembling of self-reactive TCR, IL-23R expression is still low, suggesting that assembled TCR complex is required but is not sufficient to induce IL-23-mediated thymocyte apoptosis. A second requirement is signaling through the IL-23R/RORγt pathway which forms a positive feedback loop since IL-23R expression was diminished in $Rorc^{+/-}$ heterozygote mice compared to $Rorc^{+/+}$ homozygote mice. Thymocyte co-culture in the presence of IL-23 plus self Ag *in vitro* resulted in further upregulation of IL-23R/RORγt signaling which lead to IL-23 mediated apoptosis. We therefore propose that under naïve condition, engagement of the TCR complex by self-antigen is a key predisposing factor and IL-23 may act as a second regulatory mechanism to enhance the susceptibility of weakly self-reactive $CD4^{hi}CD8^{hi}$ late-stage DP thymocytes to apoptosis.

Most thymic cells are able to produce cytokines either spontaneously or after stimulation [47]. Various groups have demonstrated previously that the production of cytokines, such as IL-7 [48,49] by thymic epithelial cells, IL-12 [50] by thymic dendritic cells as well as IFNγ [51,52], IL-4 [53–55] and IL-2 [12,56] by thymocytes, affects thymocyte development and differentiation. Significant reduction of DP thymocytes was also reported previously under other inflammatory conditions including dextran-sulfate sodium-induced colitis [57–59]. We do not completely rule out the involvement of other cytokines in the massive apoptosis found in *Aspergillus fumigatus*-infected mice, although the results suggested that IL-23, in combination with TCR signaling that occurs at the $CD4^{hi}CD8^{hi}$ late-stage of DP thymocyte development, plays an important role in this process. Increasing evidence suggests that thymic conventional DCs (cDC) but not plasmacytoid DCs (pDC) cross-present self-antigens to developing thymocytes and play an important role in thymocyte negative selection and central tolerance induction. All these are consistent with recent finding that $CD103^+$ DCs are the major source of intrathymic IL-23[60].

Our data show for the first time that IL-23 is involved in thymic negative selection. How this process affects multiple cells in the periphery of the host in resolving fungal infection is not precisely known. However, as IL-23R signaling in $CD4^+$ T cells induces effector T_H-17 [61,62] and suppresses regulatory $CD4^+$ T cells [40] in the periphery, our findings suggest a potential IL-23 mediated central immune regulation mechanism that may promote inflammation by limiting thymic regulatory T cell output. Increased understanding of this process may lead to novel approaches beneficial for control of infection and systemic autoimmune diseases.

Methods

Mice

Il23 p19$^{-/-}$ mice were obtained from Merck Research Laboratory (Palo Alto, CA.) [24,25]. The IL-23R-GFP KI mouse and the homozygous *Il23r*$^{-/-}$ mouse were obtained from the Department of Pediatrics, University of Washington, Seattle, WA [36]. WT B6, B6 C.Cg-*Foxp3*^{tm2Tch}/J and B6.129P2(Cg)-*Rorc*^{tm2Litt}/J [63] mice were obtained from Jackson Laboratory (Bar Harbor, ME) and D^{b}/H-Y Tg from Taconic Farms (Hudson, NY). C57BL/6 CD45.1 (Ly5.1) mice were purchased from the UAB Gnotobiotic Facility. All mice were kept in the animal facilities of University of Alabama at Birmingham, AL under specific pathogen-free conditions until used for the experiments. All experiments conducted in this study have been reviewed and approved by the institutional animal care and use committee of University of Alabama at Birmingham. All mice were 6–12 weeks-old female unless otherwise indicated.

Preparation of *Aspergillus fumigatus* and *in vivo* challenge

Aspergillus fumigatus isolate 13073 was cultured on potato dextrose agar at 37°C for 7 days and harvested was harvested with a cell scraper, and enumerated using a hemocytometer. 5 × 10^{7} *Aspergillus fumigatus* conidia were administrated to each mouse in a volume of 100 μl by Intraperitoneal injection.

Bone marrow transplantation

Indicated recipients were sublethally γ-irradiated (320 rads) and reconstituted with indicated donor bone marrow cells. Bone marrow cells from donor mice (2 × 10^{7}) were injected into each recipient mouse by I.V. administration 30 min after irradiation. After irradiation, the mice are kept on acidic, antibiotic water for 2 weeks (Water is first adjusted to pH 2.6 with concentrated HCl and autoclaved in 1L bottles. Then, to 1L of acidic H_2O, add 10 ml of 10 mg/ml neomycin in saline (Sigma N112, 20 ml vials). Animals were allowed to recover for at least five weeks.

Administration of adenvirus and z-VAD

For the AdIL-23 producing high expression of IL-23 and the control AdLacZ, AdIL-23 (2×10^{9} p.f.u. per mouse; a generous gift from Dr. Jay K. Kolls at the Louisiana State University Health Sciences Center made by Dr. Euan Lockhart) [34,35] or AdLacZ (2×10^{9} p.f.u. per mouse) was administered intravenously (i.v.). z-VAD (200 μg per mouse, R&D) were given by I.V. injection 24 hrs after AdIL-23 administration.

Thymus collection and cell count

The thymus was removed and immediately placed in RPMI 1640 medium. Thymi were photographed using a Cool PIX990 digital camera (Nikon, Tokyo, Japan). Single cell suspensions were obtained after 1% collagenase D (Roche Applied Science, Indianapolis, IN) digestion of whole thymi at 37°C for 30min. Thymocyte count was determined using a Cellometer Auto T4 Plus Cell Counter (Nexcelom Biosciences LLC, Lawrence, MA).

Flow cytometry analysis

Single-cell suspensions of thymocytes were analyzed by flow cytometry using combinations of PE-Cy7 anti-mouse CD90.2 (Thy-1.2) (1:400 dilution, clone 53-2.1), A700 or APC-anti-CD4 (1:400 dilution, clone H129.19), PE-anti-mouse H-Y TCR (1: 200 dilution, clone T3.70, eBioscience, CA), pacific blue anti-mouse CD8 (1:400 dilution, clone 53-6.7), PE-anti-mouse/human Foxp3 (1:50 dilution, clone 150D), APC-anti-mouse/human Helios (1:50 dilution, clone 22F6), Biotin anti-mouse CD3ε Antibody(1:400 dilution, clone 145-2C11), Biotin anti- mouse TCR αβ (1:400 dilution, clone WT31, BD PharMingen, San Diego, CA), Biotin-conjugated anti-CD11c (1:100 dilution, clone N418), APC-anti-human/mouse RORγt (1:100 dilution, clone AFKJS-9, eBioscience, CA) and Anti-IL23R antibody as primary antibody (1:100 dilution, Goat polyclonal to IL23 Receptor, Abcam, CA), Alexa Fluor® 488 donkey anti-goat IgG (H+L) (1:200 dilution, Invitrogen, CA) as secondary antibody for IL-23R staining. Unless specified, all antibodies used for FACS staining were obtained from Biolegend (San Diego, CA). Single-cell suspensions of thymocytes were washed once with FACS buffer (5% FCS and 0.1% sodium azide in PBS), and incubated first with unconjugated anti-CD16/CD32 (1:200 dilution, Fc Block; BD PharMingen, San Diego, CA) at room temperature for 20 min. Cells were then incubated with a biotin-conjugated Ab at room temperature for 20 min and washed once with FACS buffer. Second-step incubations were performed at room temperature for 20 min with pacific blue, APC-Cy7-streptavidin, PE-, PE-Cy7-, APC- and FITC-conjugated Abs. Intracellular staining for RORγt was performed using the One-step kit for nuclear proteins (eBioscience, San Diego, CA). After staining, the cells were washed twice with FACS buffer and stainingstored in PBS containing 2% paraformaldehyde until FACS analysis. Cells (300,000/sample) were analyzed on an LSRII Flow Cytometry Analyzer (BD Biosciences, Franklin Lakes, NJ).

Histology analysis

The thymi were removed from the mice immediately after sacrifice, fixed in 10% phosphate-buffered formalin (pH 7.0), and embedded in paraffin. Thin tissue sections (7 nm) were cut, deparaffinated, and stained with H&E.

Immunohistochemical staining

Tissue samples of the thymi of sacrificed mice were collected and fixed in 10% neutral formalin. Before Paraffin sections obtained were stained, endogenous peroxidase activity was suppressed by incubating the slides in 3% H_2O_2 for 5 min. Sections were incubated in PBE buffer (PBS containing 1% BSA, 1 mM EDTA, and 0.15 mM NaN3, pH 7.6) with 1% goat serum for 20 min to reduce nonspecific staining. The sections were then incubated for 60 min with the purified rat anti-mouse S100 (1:50 dilution, Clone 6G1, BD Biosciences) diluted in PBE buffer. The secondary reagents were revealed using streptavidin peroxidase (Signet, Dedham, MA), which was applied for 20 min. The diaminobenzidine (DAB) substrate reagent (BioGenex, San Ramon, CA) was prepared immediately before use and applied for 7 min. The stained sections were lightly counterstained with hematoxylin before mounting. In all cases, negative controls, consisting of incubations without the primary Ab, were included in the analyses.

TUNEL staining

TUNEL staining was performed using an ApopTag In Situ Apoptosis Staining kit on paraffin embedded sections (Serologicals, Norcross, GA)[63,64]. Deparaffinize Tissues were quenched in 3.0% hydrogen peroxide for endogenous peroxidase first and then incubate in a humidified chamber at 37°C for 1 hour with working Strength TdT Enzyme. Anti-Digoxigenin conjugate and peroxidase substrate were applied separately for 30 minutes before mounting.

Ki67 staining

Thymi were collected and fixed in 10% neutral formalin. Paraffin sections obtained were stained with primary antibodies for Ki-67 (1:50 dilution, Laboratory Vision Corporation, Fremont, California). The slides were heated in a 10mM EDTA solution at pH 8 in a pressure cooker for 10 minutes and then cooled slowly. Negative controls were performed by omitting the primary antibodies. Secondary detection was accomplished using a multispecies detection system (Signet Laboratories Inc, Dedham, Massachusetts). The sections were exposed to a biotinylated anti-mouse antibody (1:100 dilution) for 20 minutes and then peroxidase-labeled streptavidin (1:100 dilution) was added for 20 minutes. A diaminobenzidine tetrachloride supersensitive substrate kit (BioGenex) was used to visualize the antibody-antigen complex. Each section was counterstained using a weak Myers hematoxylin, dehydrated using graded alcohols, and soaked in xylene baths.

Frozen fluorescence staining

Tissue samples of the thymi of sacrificed mice were embedded in Histo-Prep frozen tissue embedding medium (Fisher Scientific, Fairlawn, NJ) and snap-frozen on dry ice. Frozen sections of thymic tissue were fixed in acetone for 15 min before staining. Sections were incubated in PBE buffer (PBS containing 1% BSA, 1 mM EDTA, and 0.15 mM NaN3, pH 7.6) with 1% horse serum for 20 min to reduce nonspecific staining. The sections were then incubated for 30 min with A647 anti-CD90.2 (1:100 dilution, clone 30-H12, Biolegend) and purified anti-EpCAM (clone G8.8, eBioscience) conjugated with A555 by APEX™ Alex Fluor® 555 Antibody Labeling Kit (Invitorgen, CA). In all cases, negative controls, consisting of incubations without the primary Ab, were included in the analyses.

Histomorphometry Quantitation

BioQuant® Image Analysis software (R&M Biometrics, Nashville, TN) was used for histomorphometrical analyses as we previously described [24]. On H&E-stained sections (at 5×), area measurements were made of the total tissue area (area enclosed by the outline of the whole section), cortical area and medullary area (areas distinguished by the difference of the histological appearance and stained color). Percentages of cortical area and medullary area per total tissue area were calculated using the formula: (cortical area/total tissue area) ×100; and (medullary area/total tissue area) ×100. On TUNEL and Ki67 immunohistochemistry stained sections (at 5×), area measurements were made of the total tissue areas (area enclosed by the outline of the TUNEL stained section or Ki67 stained section), TUNEL positive, and Ki67 positive areas (areas measured by picking the pixels with brown color from DAB chromogen on both sections, using BioQuant's thresholding

tool). Percentages of TUNEL$^+$ and Ki67$^+$ area per total tissue area were calculated using the formula: (TUNEL$^+$ area/total tissue area) ×100, and (Ki67$^+$ area/total tissue area) ×100.

SYBR green real-time quantitative RT-PCR analysis

RNA isolated from the thymus of 2-mo-old mice (five samples per group) was used to construct cDNA using the Maxima® First Strand cDNA Synthesis Kit (Fermentas Inc., Glen Burnie, MD). The sequence of the primers used were:

Bcl-xl sense: GAGCAGGTAGTGAATGAAC, *Bcl-xl* anti-sense: GATCCAAGGCTCTAGGTG; *Il2* sense: GAAGGCTATCCATCTCCTCAG, *c-Rel* anti-sense: CCTGACACTTCCACAGTTCTTG; *Il23* sense: AGTGTGAAGATGGTTGTGAC,

Il23 anti-sense: CTGGAGGAGTTGGCTGAG; *Il23r* sense: CACTGCTGAATGAATGTCCTGGTC; *Il23r* anti-sense: GGTATCTATGTAGGTAGGCTTCC; *Rorc* sense: TTCTCATCAATGCCAACCG,

Rorc anti-sense: GCCAGTTCCAAATTGTATTGC; *Gapdh* sense: AGGTCGGTGTGAACGGATTTG, *Gapdh* anti-sense: TGTAGACCATGTAGTTGAGGTCA.

All probes were designed to span an intron to prevent amplification of DNA potentially present in the sample.

In each run, serial of 10-fold dilutions of a single standard cDNA derived from a positive control mouse RNA (Stratagene, La Jolla, CA) were amplified to create a standard curve, and values of unknown samples were estimated relative to this standard curve. Replicate dilutions of the unknown sample cDNAs from 40 ng of total RNA were combined with a mixture of primers, iQ SYBR Green Supermix with Taq polymerase, and nucleotides (Bio-Rad). Each sample (total volume, 25 μl) was assayed in an optical tube designed for the 96-well format for the IQ5 Thermocycler (Bio-Rad). Each PCR amplification was performed in duplicate using the following conditions: 5 min at 94°C, followed by a total of 40 cycles (15 s at 94°C and 30 s at 55°C). Each PCR was run in duplicate. The mean value of the two reactions was defined as representative of the sample. The volumes described above yielded standard curves with a linear relationship between the copy number of the original internal standard added and the number of PCR cycles required to exceed a preset threshold according to the method described by Dreskin et al [65]. From these standard curves, the relative amount of cDNA for the house keeping gene *Gapdh* and the relative amount of cDNA for each gene were determined for each sample.

Thymocyte stimulation assay

Thymocytes were cultured in triplicate with IL-2 (5 ng/ml, eBioscience, CA) and IL-7 (5 ng/ml, R&D, MN), with or without purified mouse rIL-23 (R&D, 20 ng/ml) or irradiated (3200 Rads) splenocytes from male or female Thy1.1 mice as stimulator (ratio: stimulators/responders=1/3) for 20 h. Flow cytometry analysis were performed for the expression of the indicated markers. Apoptosis was quantitated using 7-amino actinomycin D (7-AAD) staining and was accessed by flow cytometry [51].

Statistical analysis

The values are reported as the mean of each group ± standard error of the mean (SEM). Statistical analyses were performed using Student's unpaired two-tailed *t* test. A value of $p<0.05$ was considered statistically significant.

Supplementary Material

Refer to Web version on PubMed Central for supplementary material.

Acknowledgments

We thank Drs. J. Kolls (Louisiana State University)and Paul Robbins (University of Pittsburgh) for providing AdLacZ and AdIL-23; Dr. N. Manley (University of Georgia) for technical support in the TEC sorting; and Dr. F. Hunter for review of the manuscript. Flow cytometry and confocal imaging data acquisition were carried out at the UAB Comprehensive Flow Cytometry Core (P30 AR048311 and P30 AI027767) and UAB Analytic Imaging and Immunoreagent Core (P30 AR048311) respectively; BioQuant histomorphometry analysis was carried out at the UAB Center for Metabolic Bone Disease-Histomorphometry and Molecular Analysis Core Laboratory (P30 AR46031). This work is supported by grants from VA Merit Review Grant (1I01BX000600-01), NIH/NIAID (1AI 071110, ARRA 3RO1AI71110-02S1 and 1RO1 AI083705), Rheumatology Research Foundation, Lupus Research Institute, and Arthritis Foundation.

References

1. Saito T, Watanabe N. Positive and negative thymocyte selection. Crit Rev Immunol. 1998; 18:359–370. [PubMed: 9704194]
2. Bouvier G, et al. Deletion of the mouse T-cell receptor beta gene enhancer blocks alphabeta T-cell development. Proc Natl Acad Sci U S A. 1996; 93:7877–7881. [PubMed: 8755570]
3. Fowlkes BJ, Schwartz RH, Pardoll DM. Deletion of self-reactive thymocytes occurs at a CD4+8+ precursor stage. Nature. 1988; 334:620–623.10.1038/334620a0 [PubMed: 3261392]
4. White H, Bergmann G. Localization in near-monolayer films. Phys Rev B Condens Matter. 1989; 40:11594–11602. [PubMed: 9991759]
5. Wu L, Shortman K. Heterogeneity of thymic dendritic cells. Semin Immunol. 2005; 17:304–312. S1044-5323(05)00039-4 [pii]. 10.1016/j.smim.2005.05.001 [PubMed: 15946853]
6. Goldschneider I, Cone RE. A central role for peripheral dendritic cells in the induction of acquired thymic tolerance. Trends Immunol. 2003; 24:77–81. S1471490602000388 [pii]. [PubMed: 12547504]
7. Heino M, et al. RNA and protein expression of the murine autoimmune regulator gene (Aire) in normal, RelB-deficient and in NOD mouse. Eur J Immunol. 2000; 30:1884–1893. [pii]10.1002/1521-4141(200007)30:7<1884::AID-IMMU1884>3.0.CO;2-P. 10.1002/1521-4141(200007)30:7<1884::AID-IMMU1884>3.0.CO;2-P [PubMed: 10940877]
8. He YW, Deftos ML, Ojala EW, Bevan MJ. RORgamma t, a novel isoform of an orphan receptor, negatively regulates Fas ligand expression and IL-2 production in T cells. Immunity. 1998; 9:797–806. S1074-7613(00)80645-7 [pii]. [PubMed: 9881970]
9. Kurebayashi S, et al. Retinoid-related orphan receptor gamma (RORgamma) is essential for lymphoid organogenesis and controls apoptosis during thymopoiesis. Proc Natl Acad Sci U S A. 2000; 97:10132–10137. 97/18/10132 [pii]. [PubMed: 10963675]
10. Sun Z, et al. Requirement for RORgamma in thymocyte survival and lymphoid organ development. Science. 2000; 288:2369–2373. [PubMed: 10875923]
11. Littman DR, et al. Role of the nuclear hormone receptor ROR gamma in transcriptional regulation, thymocyte survival, and lymphoid organogenesis. Cold Spring Harb Symp Quant Biol. 1999; 64:373–381. [PubMed: 11232310]
12. Bassiri H, Carding SR. A requirement for IL-2/IL-2 receptor signaling in intrathymic negative selection. J Immunol. 2001; 166:5945–5954. [PubMed: 11342609]

13. Liou HC, Smith KA. The roles of c-rel and interleukin-2 in tolerance: a molecular explanation of self-nonself discrimination. Immunol Cell Biol. 89:27–32. icb2010120 [pii]. 10.1038/icb.2010.120 [PubMed: 20975733]
14. He YW, et al. Down-regulation of the orphan nuclear receptor ROR gamma t is essential for T lymphocyte maturation. J Immunol. 2000; 164:5668–5674. ji_v164n10p5668 [pii]. [PubMed: 10820242]
15. Oppmann B, et al. Novel p19 protein engages IL-12p40 to form a cytokine, IL-23, with biological activities similar as well as distinct from IL-12. Immunity. 2000; 13:715–725. S1074-7613(00)00070-4 [pii]. [PubMed: 11114383]
16. Kastelein RA, Hunter CA, Cua DJ. Discovery and biology of IL-23 and IL-27: related but functionally distinct regulators of inflammation. Annu Rev Immunol. 2007; 25:221–242.10.1146/annurev.immunol.22.012703.104758 [PubMed: 17291186]
17. Tato CM, Cua DJ. Reconciling id, ego, and superego within interleukin-23. Immunol Rev. 2008; 226:103–111. IMR715 [pii]. 10.1111/j.1600-065X.2008.00715.x [PubMed: 19161419]
18. Ivanov, et al. The orphan nuclear receptor RORgammat directs the differentiation program of proinflammatory IL-17+ T helper cells. Cell. 2006; 126:1121–1133. S0092-8674(06)01105-6 [pii]. 10.1016/j.cell.2006.07.035 [PubMed: 16990136]
19. Wilson NJ, et al. Development, cytokine profile and function of human interleukin 17-producing helper T cells. Nat Immunol. 2007; 8:950–957. ni1497 [pii]. 10.1038/ni1497 [PubMed: 17676044]
20. Werner JL, et al. Neutrophils produce interleukin 17A (IL-17A) in a dectin-1- and IL-23-dependent manner during invasive fungal infection. Infect Immun. 2011; 79:3966–3977.10.1128/IAI.05493-11 [PubMed: 21807912]
21. Gessner MA, et al. Dectin-1-dependent interleukin-22 contributes to early innate lung defense against Aspergillus fumigatus. Infect Immun. 2012; 80:410–417.10.1128/IAI.05939-11 [PubMed: 22038916]
22. Gafa V, et al. Human dendritic cells following Aspergillus fumigatus infection express the CCR7 receptor and a differential pattern of interleukin-12 (IL-12), IL-23, and IL-27 cytokines, which lead to a Th1 response. Infect Immun. 2006; 74:1480–1489.10.1128/IAI.74.3.1480-1489.2006 [PubMed: 16495518]
23. Chen Y, et al. Anti-IL-23 therapy inhibits multiple inflammatory pathways and ameliorates autoimmune encephalomyelitis. J Clin Invest. 2006; 116:1317–1326.10.1172/JCI25308 [PubMed: 16670771]
24. Cua DJ, et al. Interleukin-23 rather than interleukin-12 is the critical cytokine for autoimmune inflammation of the brain. Nature. 2003; 421:744–748.10.1038/nature01355 [PubMed: 12610626]
25. Murphy CA, et al. Divergent pro- and antiinflammatory roles for IL-23 and IL-12 in joint autoimmune inflammation. J Exp Med. 2003; 198:1951–1957.10.1084/jem.20030896 [PubMed: 14662908]
26. Kyttaris VC, Zhang Z, Kuchroo VK, Oukka M, Tsokos GC. Cutting edge: IL-23 receptor deficiency prevents the development of lupus nephritis in C57BL/6-lpr/lpr mice. J Immunol. 2010; 184:4605–4609.10.4049/jimmunol.0903595 [PubMed: 20308633]
27. Kisielow P, Bluthmann H, Staerz UD, Steinmetz M, von Boehmer H. Tolerance in T-cell-receptor transgenic mice involves deletion of nonmature CD4+8+ thymocytes. Nature. 1988; 333:742–746.10.1038/333742a0 [PubMed: 3260350]
28. Bluthmann H, et al. T-cell-specific deletion of T-cell receptor transgenes allows functional rearrangement of endogenous alpha- and beta-genes. Nature. 1988; 334:156–159.10.1038/334156a0 [PubMed: 3260351]
29. von Boehmer H, Teh HS, Kisielow P. The thymus selects the useful, neglects the useless and destroys the harmful. Immunol Today. 1989; 10:57–61. [PubMed: 2526642]
30. Farr AG, Dooley JL, Erickson M. Organization of thymic medullary epithelial heterogeneity: implications for mechanisms of epithelial differentiation. Immunol Rev. 2002; 189:20–27. imr18903 [pii]. [PubMed: 12445262]
31. Chen L, Xiao S, Manley NR. Foxn1 is required to maintain the postnatal thymic microenvironment in a dosage-sensitive manner. Blood. 2009; 113:567–574. blood-2008-05-156265 [pii]. 10.1182/blood-2008-05-156265 [PubMed: 18978204]

32. Bettelli E, et al. Reciprocal developmental pathways for the generation of pathogenic effector TH17 and regulatory T cells. Nature. 2006; 441:235–238. nature04753 [pii]. 10.1038/nature04753 [PubMed: 16648838]
33. Veldhoen M, Hocking RJ, Atkins CJ, Locksley RM, Stockinger B. TGFbeta in the context of an inflammatory cytokine milieu supports de novo differentiation of IL-17-producing T cells. Immunity. 2006; 24:179–189. S1074-7613(06)00004-5 [pii]. 10.1016/j.immuni.2006.01.001 [PubMed: 16473830]
34. Happel KI, et al. Cutting edge: roles of Toll-like receptor 4 and IL-23 in IL-17 expression in response to Klebsiella pneumoniae infection. J Immunol. 2003; 170:4432–4436. [PubMed: 12707317]
35. Reay J, Kim SH, Lockhart E, Kolls J, Robbins PD. Adenoviral-mediated, intratumor gene transfer of interleukin 23 induces a therapeutic antitumor response. Cancer Gene Ther. 2009; 16:776–785. cgt200927 [pii]. 10.1038/cgt.2009.27 [PubMed: 19390568]
36. Awasthi A, et al. Cutting edge: IL-23 receptor gfp reporter mice reveal distinct populations of IL-17-producing cells. J Immunol. 2009; 182:5904–5908. 182/10/5904 [pii]. 10.4049/jimmunol.0900732 [PubMed: 19414740]
37. Sprent J, Kosaka H, Gao EK, Surh CD, Webb SR. Intrathymic and extrathymic tolerance in bone marrow chimeras. Immunol Rev. 1993; 133:151–176. [PubMed: 8225365]
38. Ron Y, Lo D, Sprent J. T cell specificity in twice-irradiated F1----parent bone marrow chimeras: failure to detect a role for immigrant marrow-derived cells in imprinting intrathymic H-2 restriction. J Immunol. 1986; 137:1764–1771. [PubMed: 2943799]
39. Takada A, Takada Y, Huang CC, Ambrus JL. Biphasic pattern of thymus regeneration after whole-body irradiation. J Exp Med. 1969; 129:445–457. [PubMed: 4886041]
40. Ahern PP, et al. Interleukin-23 drives intestinal inflammation through direct activity on T cells. Immunity. 2010; 33:279–288.10.1016/j.immuni.2010.08.010 [PubMed: 20732640]
41. McGeachy MJ, Cua DJ. The link between IL-23 and Th17 cell-mediated immune pathologies. Semin Immunol. 2007; 19:372–376.10.1016/j.smim.2007.10.012 [PubMed: 18319054]
42. McGeachy MJ, et al. The interleukin 23 receptor is essential for the terminal differentiation of interleukin 17-producing effector T helper cells in vivo. Nat Immunol. 2009; 10:314–324.10.1038/ni.1698 [PubMed: 19182808]
43. Petermann F, et al. gammadelta T cells enhance autoimmunity by restraining regulatory T cell responses via an interleukin-23-dependent mechanism. Immunity. 2010; 33:351–363.10.1016/j.immuni.2010.08.013 [PubMed: 20832339]
44. Palmer E, Naeher D. Affinity threshold for thymic selection through a T-cell receptor-co-receptor zipper. Nat Rev Immunol. 2009; 9:207–213. nri2469 [pii]. 10.1038/nri2469 [PubMed: 19151748]
45. Gallegos AM, Bevan MJ. Central tolerance: good but imperfect. Immunol Rev. 2006; 209:290–296. IMR348 [pii]. 10.1111/j.0105-2896.2006.00348.x [PubMed: 16448550]
46. He YW. The role of orphan nuclear receptor in thymocyte differentiation and lymphoid organ development. Immunol Res. 2000; 22:71–82. IR:22:2-3:71 [pii]. 10.1385/IR:22:2-3:71 [PubMed: 11339367]
47. Yarilin AA, Belyakov IM. Cytokines in the thymus: production and biological effects. Curr Med Chem. 2004; 11:447–464. [PubMed: 14965226]
48. Fernandez E, et al. Establishment and characterization of cloned human thymic epithelial cell lines. Analysis of adhesion molecule expression and cytokine production. Blood. 1994; 83:3245–3254. [PubMed: 7514905]
49. Moore TA, von Freeden-Jeffry U, Murray R, Zlotnik A. Inhibition of gamma delta T cell development and early thymocyte maturation in IL-7 −/− mice. J Immunol. 1996; 157:2366–2373. [PubMed: 8805634]
50. Ludviksson BR, Ehrhardt RO, Strober W. Role of IL-12 in intrathymic negative selection. J Immunol. 1999; 163:4349–4359. ji_v163n8p4349 [pii]. [PubMed: 10510375]
51. Galy AH, Spits H. IL-1, IL-4, and IFN-gamma differentially regulate cytokine production and cell surface molecule expression in cultured human thymic epithelial cells. J Immunol. 1991; 147:3823–3830. [PubMed: 1719090]

52. Patel DD, Whichard LP, Radcliff G, Denning SM, Haynes BF. Characterization of human thymic epithelial cell surface antigens: phenotypic similarity of thymic epithelial cells to epidermal keratinocytes. J Clin Immunol. 1995; 15:80–92. [PubMed: 7559912]

53. Kuhn R, Rajewsky K, Muller W. Generation and analysis of interleukin-4 deficient mice. Science. 1991; 254:707–710. [PubMed: 1948049]

54. Zlotnik A, Ransom J, Frank G, Fischer M, Howard M. Interleukin 4 is a growth factor for activated thymocytes: possible role in T-cell ontogeny. Proc Natl Acad Sci U S A. 1987; 84:3856–3860. [PubMed: 3495799]

55. Tepper RI, et al. IL-4 induces allergic-like inflammatory disease and alters T cell development in transgenic mice. Cell. 1990; 62:457–467. 0092-8674(90)90011-3 [pii]. [PubMed: 2116236]

56. Park JH, Mitnacht R, Torres-Nagel N, Hunig T. T cell receptor ligation induces interleukin (IL) 2R beta chain expression in rat CD4,8 double positive thymocytes, initiating an IL-2-dependent differentiation pathway of CD8 alpha+/beta− T cells. J Exp Med. 1993; 177:541–546. [PubMed: 8426123]

57. Savino W. The thymus is a common target organ in infectious diseases. PLoS Pathog. 2006; 2:e62.10.1371/journal.ppat.0020062 [PubMed: 16846255]

58. Savino W, Dardenne M, Velloso LA, Dayse Silva-Barbosa S. The thymus is a common target in malnutrition and infection. Br J Nutr. 2007; 98(Suppl 1):S11–16.10.1017/S0007114507832880 [PubMed: 17922946]

59. Sasaki S, Ishida Y, Nishio N, Ito S, Isobe K. Thymic involution correlates with severe ulcerative colitis induced by oral administration of dextran sulphate sodium in C57BL/6 mice but not in BALB/c mice. Inflammation. 2008; 31:319–328.10.1007/s10753-008-9081-3 [PubMed: 18696222]

60. Dudakov JA, et al. Interleukin-22 drives endogenous thymic regeneration in mice. Science. 336:91–95. science.1218004 [pii]. 10.1126/science.1218004 [PubMed: 22383805]

61. Ghoreschi K, et al. Generation of pathogenic T(H)17 cells in the absence of TGF-beta signalling. Nature. 2010; 467:967–971.10.1038/nature09447 [PubMed: 20962846]

62. Langrish CL, et al. IL-23 drives a pathogenic T cell population that induces autoimmune inflammation. J Exp Med. 2005; 201:233–240.10.1084/jem.20041257 [PubMed: 15657292]

63. Eberl G, et al. An essential function for the nuclear receptor RORgamma(t) in the generation of fetal lymphoid tissue inducer cells. Nat Immunol. 2004; 5:64–73. ni1022 [pii]. 10.1038/ni1022 [PubMed: 14691482]

64. Hsu HC, et al. Inhibition of the catalytic function of activation-induced cytidine deaminase promotes apoptosis of germinal center B cells in BXD2 mice. Arthritis Rheum. 63:2038–2048.10.1002/art.30257 [PubMed: 21305519]

65. Dreskin SC, et al. Measurement of changes in mRNA for IL-5 in noninvasive scrapings of nasal epithelium taken from patients undergoing nasal allergen challenge. J Immunol Methods. 2002; 268:189–195. S0022175902002065 [pii]. [PubMed: 12215387]

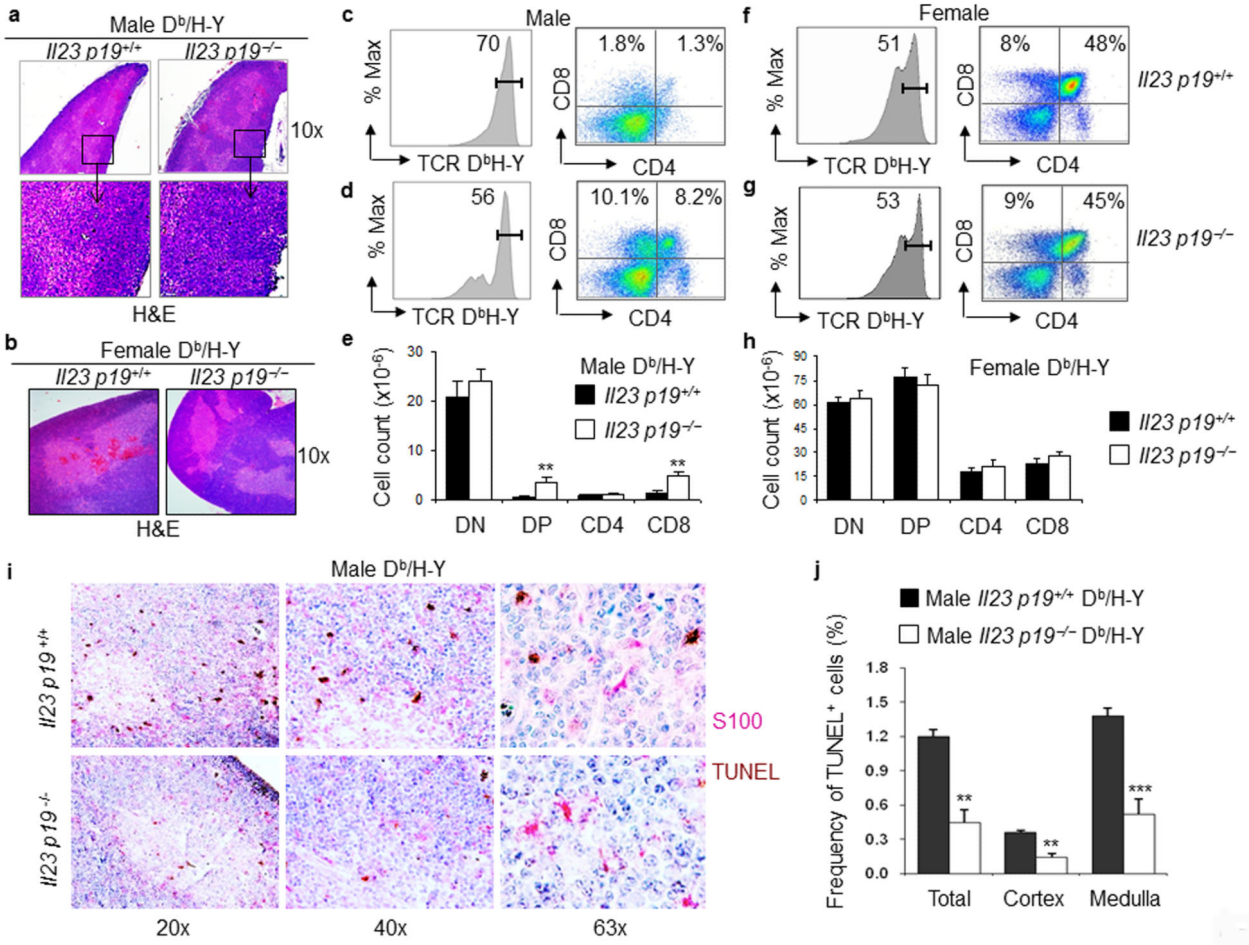

Figure 1. Decreased thymic negative selection in *Il23 p19*$^{-/-}$ mice

(**a**) H&E staining of thymus from the indicated male mice. Enlarged images of the outlined area from upper images are shown below. (**b**) H&E staining of thymus from the indicated female mice. The object lens used to acquire the images is shown. Scale bars in (a) and (b): 300 μm. (**c–h**) Flow cytometry analysis of the frequency of H-Y TCR^{+} thymocytes and the distribution of CD4/CD8 in H-Y TCR^{+} thymocytes in (**c**) male *Il23 p19*$^{+/+}$ Tg, (**d**) male *Il23 p19*$^{-/-}$ Tg, (**f**) female *Il23 p19*$^{+/+}$ Tg and (**g**) female *Il23 p19*$^{-/-}$ Tg mice. In each group, all samples were gated first on Thy1.2^{+} cells. Numbers shown within each quadrant indicate the percent cells in the quadrant. Cell counts of the indicated populations of thymocytes (**e, h**). All populations were gated within the TCR D^{b}/H-Y^{+} thymocytes. All results shown were calculated based on the percentage of each subpopulation of thymocytes multiplied by the total thymocyte count multiplied by 10^{-6}. (**i**) Immunohistochemistry staining of thymic DCs (S100^{+}, magenta) and apoptotic cells (TUNEL^{+}, dark brown). The object lens used to acquire each panel of image is shown at the bottom. Scale bar: 100 μm. (**j**) The percentage of TUNEL^{+} cells at the indicated thymic region was quanttated in five randomly chosen microscopic areas from each section. All results represent the mean ± SEM (N=2–3 mice per group for 3 independent experiments; ** p<0.01 and *** p<0.005 between *p19 Il23*$^{+/+}$ D^{b}/H-Y Tg male and *p19 Il23*$^{-/-}$ D^{b}/H-Y Tg male mice).

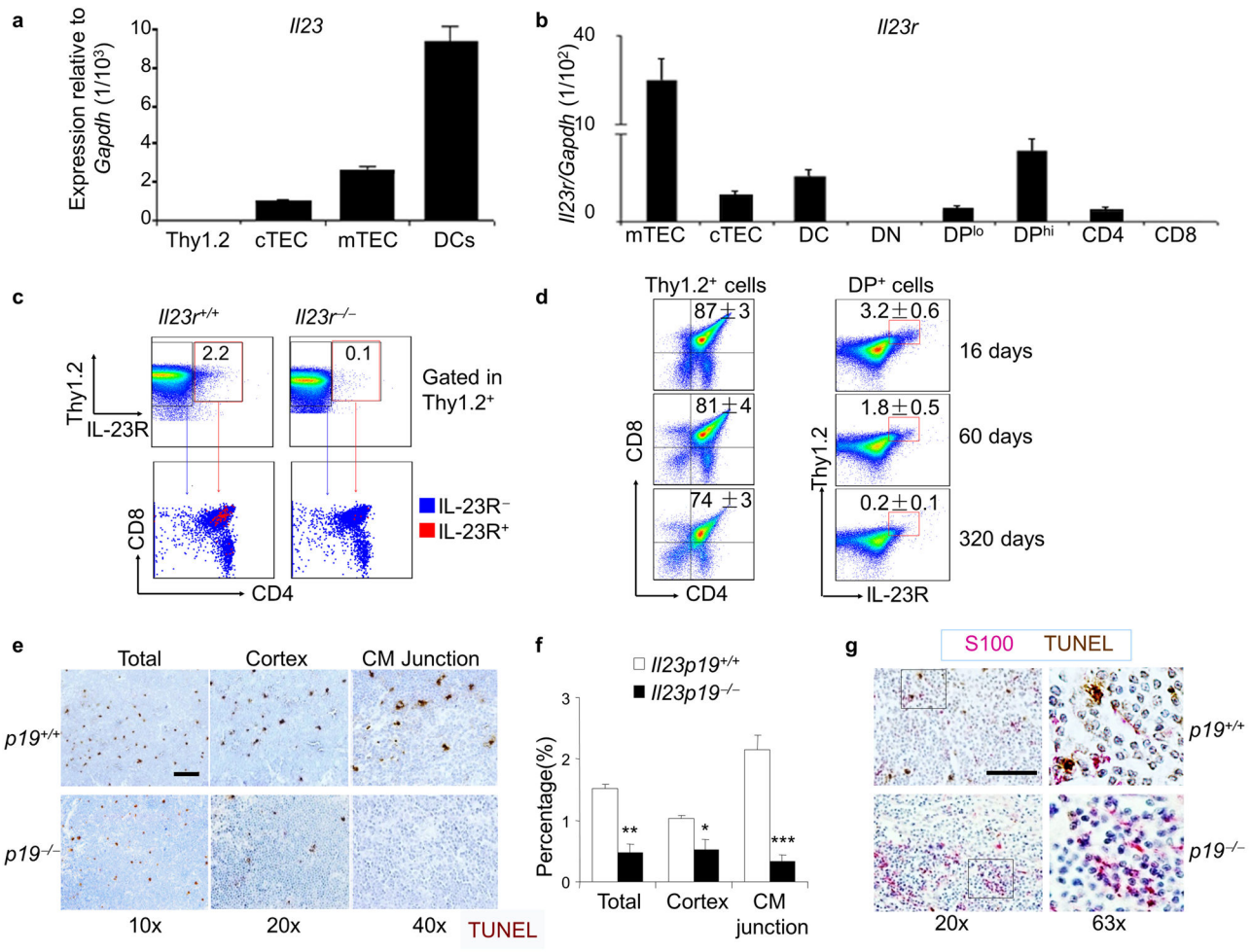

Figure 2. Decreased apoptosis in thymus of *Il23 p19*$^{-/-}$ mice

(**a, b**) qRT-PCR analysis of *Il23* (**a**) and *Il23r* (**b**) in the indicated thymic subpopulations of 2mo-old B6 mice. Data are representative of two independent experiments (mean ± SEM, N=2–3 mice per experiment). (**c**) Flow cytometry analysis of IL-23R^{+} thymocyte subpopulation distribution. Thymocytes were gated on Thy1.2^{+}IL-23R^{+} or Thy1.2^{+}IL-23R^{-} separately, each population was analyzed for expression of CD4 and CD8. (**d**) Flow cytometry analysis of IL-23R expression in CD4^{+}CD8^{+} DP thymocyte from mice of the indicated ages. Thymocytes were gated on Thy1.2^{+} population and were analyzed for expression of CD4 and CD8 (left). Cells within the DP Thy1.2^{+} subpopulation were analyzed for expression of IL-23R (right). (**e**) *In situ* TUNEL staining on thymus sections of *Il23 p19*$^{+/+}$ or *Il23 p19*$^{-/-}$ C57BL/6J mouse. The magnification of the objective lens used for each panel is shown in the bottom. (**f**) BioQuant® image analysis on the percentage of TUNEL^{+} cells. Five microscopic areas were randomly chosen for the quantitation of each section. Data in (c)–(f) are representative of three independent experiments (mean ± SEM, N=2–3 mice per group ; * p<0.05, ** p<0.01, *** p<0.005 between *Il23 p19*$^{+/+}$ and *Il23 p19*$^{-/-}$ mice). (**g**) *In situ* staining of thymic DCs and apoptotic thymocytes using S100 (magenta) and TUNEL staining (brown), respectively. The magnification of the objective lens used for each panel is shown below the images. Scale bar: 100 μm, applies to all panels.

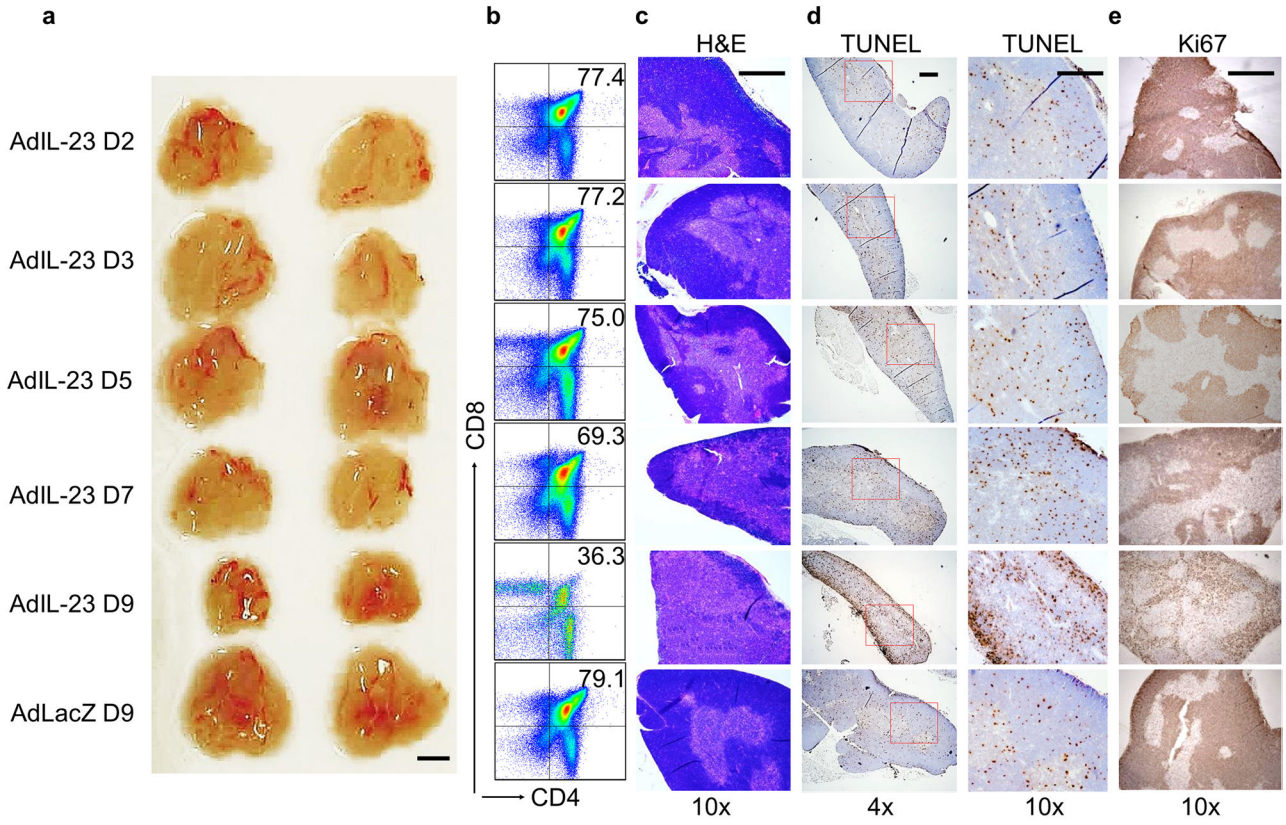

Figure 3. Delayed apoptosis induced by IL-23 in the thymus

C57BL/6 mice were injected with either AdIL-23 or AdLacZ. At the indicated day (D), mice were sacrificed. (**a**) Gross anatomical images of representative thymi from each group of mice. Scale bars: 3.0 mm. (**b**) Flow cytometry analysis of CD4 and CD8 expression on Thy1.2$^+$ cells and the percent of CD4$^+$CD8$^+$ cells is shown. (**c**) *In situ* H&E staining of a representative thymus section. (**d**) *In situ* TUNEL staining (dark brown) of a representative thymus section. (**e**) *In situ* Ki67 staining (dark brown) of a representative thymus section. The magnification of objective lens used is shown below the images. N=4–5 mice per group for 3 independent experiments. Scale bars in (c), (d) and (e): 300 μm.

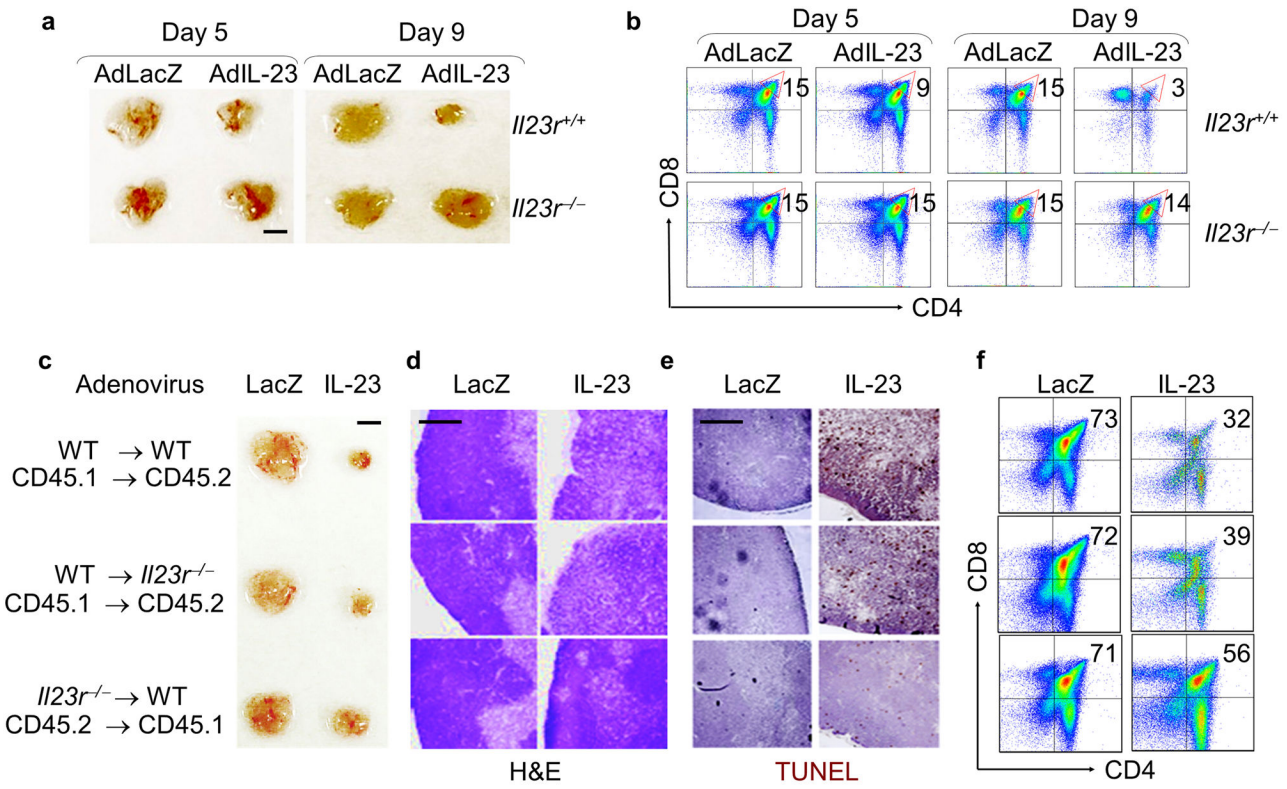

Figure 4. Induction of IL-23R for IL-23 induced thymocyte apoptosis

(**a, b**) *Il23r*$^{+/+}$ and *Il23r* $^{-/-}$ mice were administered with either AdIL-23 or AdLacZ. At the indicated time, mice were sacrificed. (**a**) Gross anatomical images of representative thymi from each group of mice. (**b**) Flow cytometry analysis of CD4 and CD8 expression on Thy1.2^{+} cells and the percent of CD4^{+}CD8^{+} cells is shown. (**c, d, e, f**) Bone marrow (BM) reconstitution was carried out in the indicated 3 groups of donor/recipient chimeric mice. Recipient mice were administered with either AdIL-23 or AdLacZ 40 days later. Mice were sacrificed after 9 days. (**c**) Gross anatomical images of representative thymi. (**d**) *In situ* H&E staining of a representative thymus section. (**e**) *In situ* TUNEL staining (dark brown) of a representative thymus section. (**f**) Flow cytometry analysis of CD4 and CD8 expression on Thy1.2^{+} cells and the percent of CD4^{+}CD8^{+} cells is shown. N=3 mice per group for 2 independent experiments. Scale bars in (a) and (c): 3.0 mm; Scale bars in (d) and (e): 300 μm.

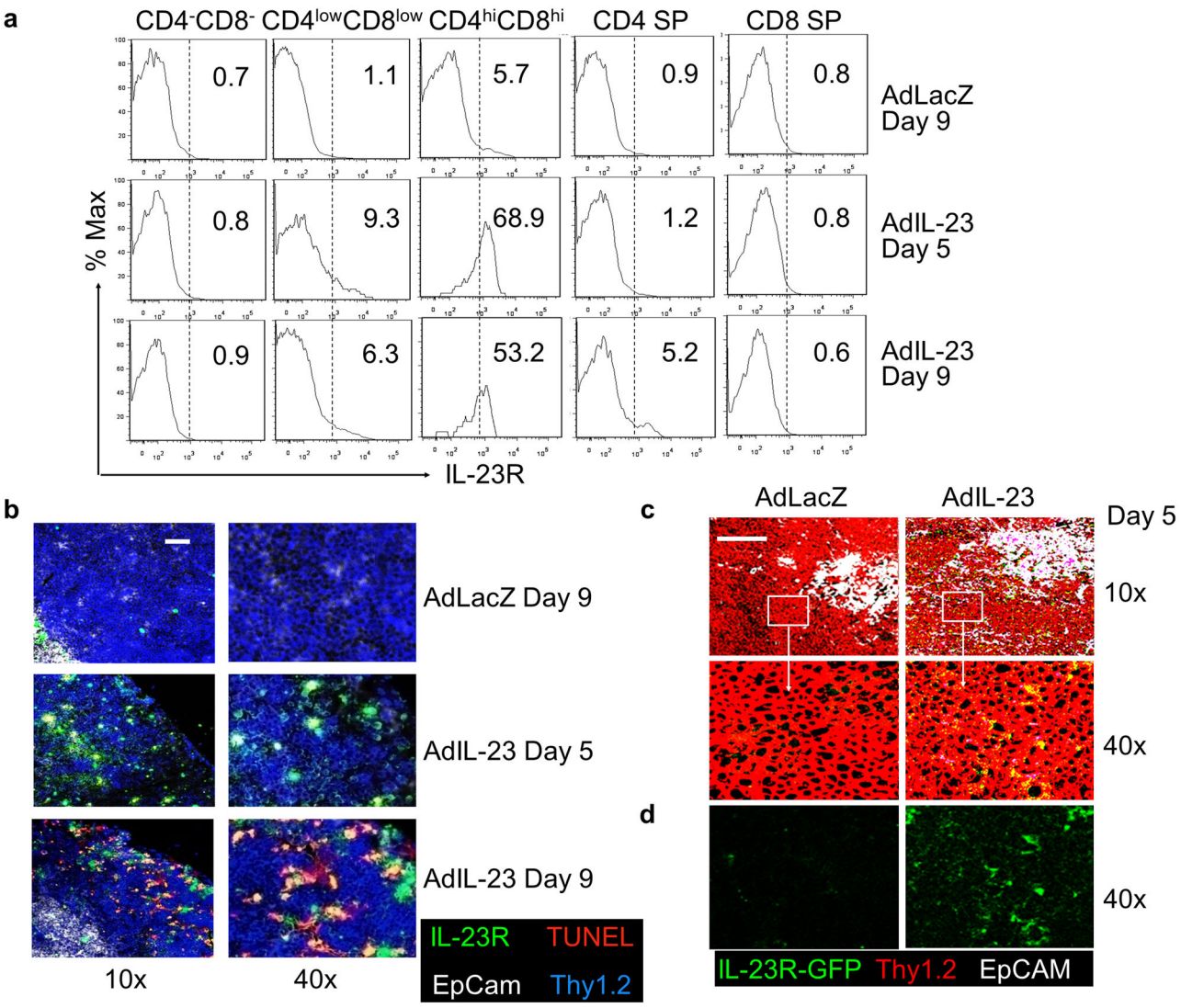

Figure 5. IL-23 upregulates IL-23R to further promote IL-23-induced apoptosis

(**a**) Flow cytometry analysis of IL-23R on the indicated thymocyte populations from WT B6 mice at the indicated times after Ad virus administration. The percent of IL-23R^{+} cells is shown. (**b**) Immunofluorescent assessment of IL-23R expression by anti-IL-23R (green) and apoptosis (TUNEL, red) of thymic sections from the indicated mice. Sections were costained with A647 anti-CD90.2 (Blue) and A555 anti-EpCAM (white). Magnification is shown below the images. (**c**) Immunofluorescent assessment of IL-23R-GFP expression (green) on thymus sections obtained from heterozygous *Il23r*$^{+/-}$-GFP KI mice 5 days after either AdLacZ or AdIL-23 administration. Sections were costained with anti-CD90.2 (red) and anti-EpCAM (white). Magnification is indicated to the right of the images. (**d**) A single green channel higher power view of the outlined area from panel c. N=4–5 mice per group for 3 independent experiments. Scale bar: 50 μm, applies to all panels.

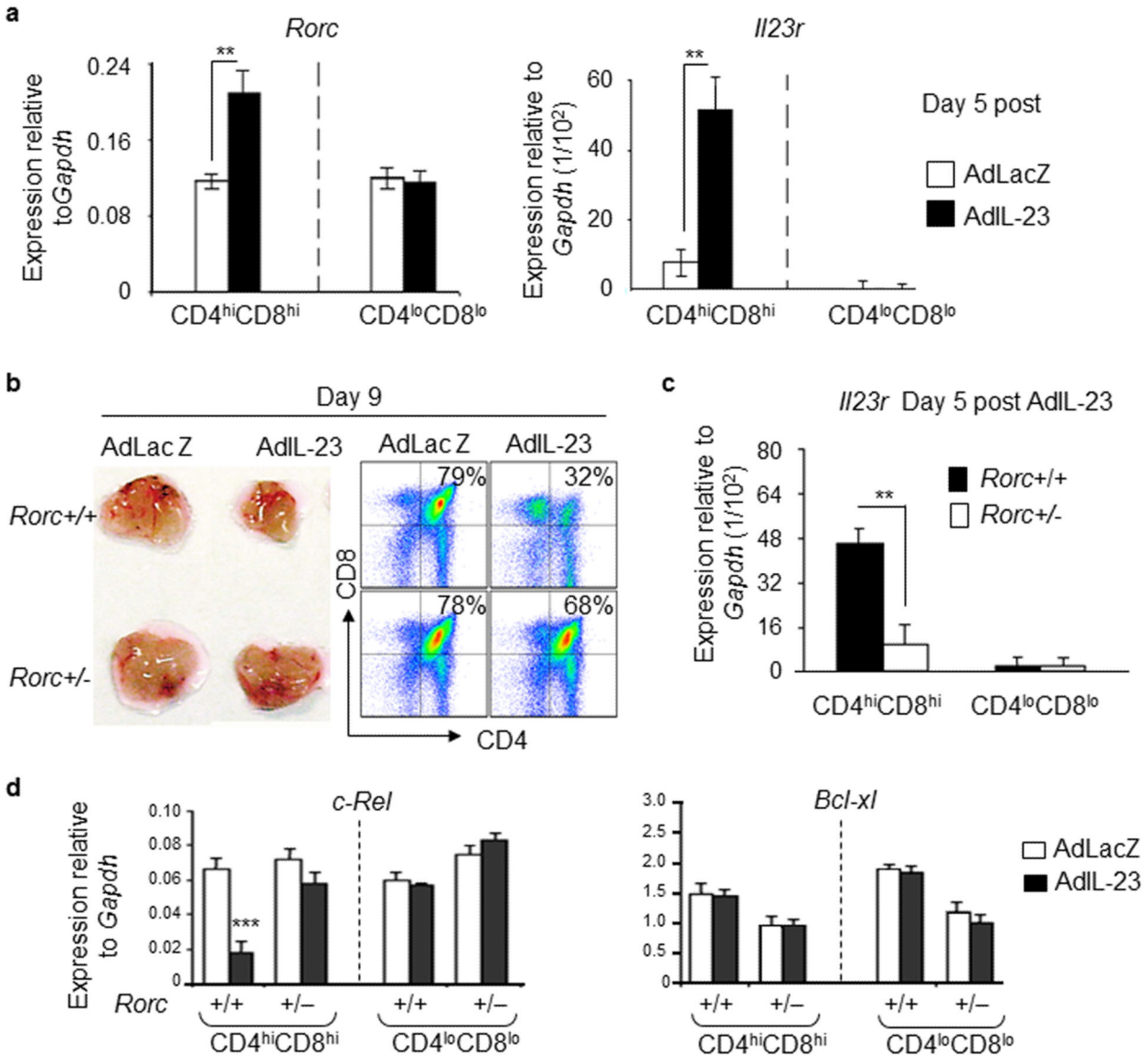

Figure 6. CD4^{hi}CD8^{hi} DP thymocytes are targets of IL-23R-RORγt mediated apoptosis

AdLacZ or AdIL-23 was administered to WT (*Rorc*$^{+/+}$) or *Rorc*$^{+/-}$ mice. (**a**) Real time qRT-PCR analysis of *Rorc* and *Il23r* on the indicated thymocytes of *Rorc*$^{+/+}$ mice at day 5. (**b**) Left: Gross anatomic images showing the size of a representative thymus of WT (*Rorc*$^{+/+}$) or *Rorc*$^{+/-}$ mice at day 9. Right: Flow cytometry analysis of CD4 and CD8 on total thymocytes (Thy1.2^{+}). The frequency of CD4^{+}CD8^{+} cells within total Thy1.2^{+} thymocytes is indicated. Scale bar: 3.0 mm. (**c**) qRT-PCR analysis of *Il23r* on the indicated thymocyte subpopulations from the indicated mouse strains at day 5. (**d**) qRT-PCR analysis of the expression of *c-Rel* and *Bcl-xl* in the indicated thymocyte subpopulations at day 5. Data in (a)–(d) are representative of three independent experiments (mean ± SEM, N=3–5 mice per group; ** p<0.01, *** p<0.005 between AdLacZ and AdIL-23 treated or *Rorc*$^{+/-}$ and *Rorc*$^{+/+}$ mice).

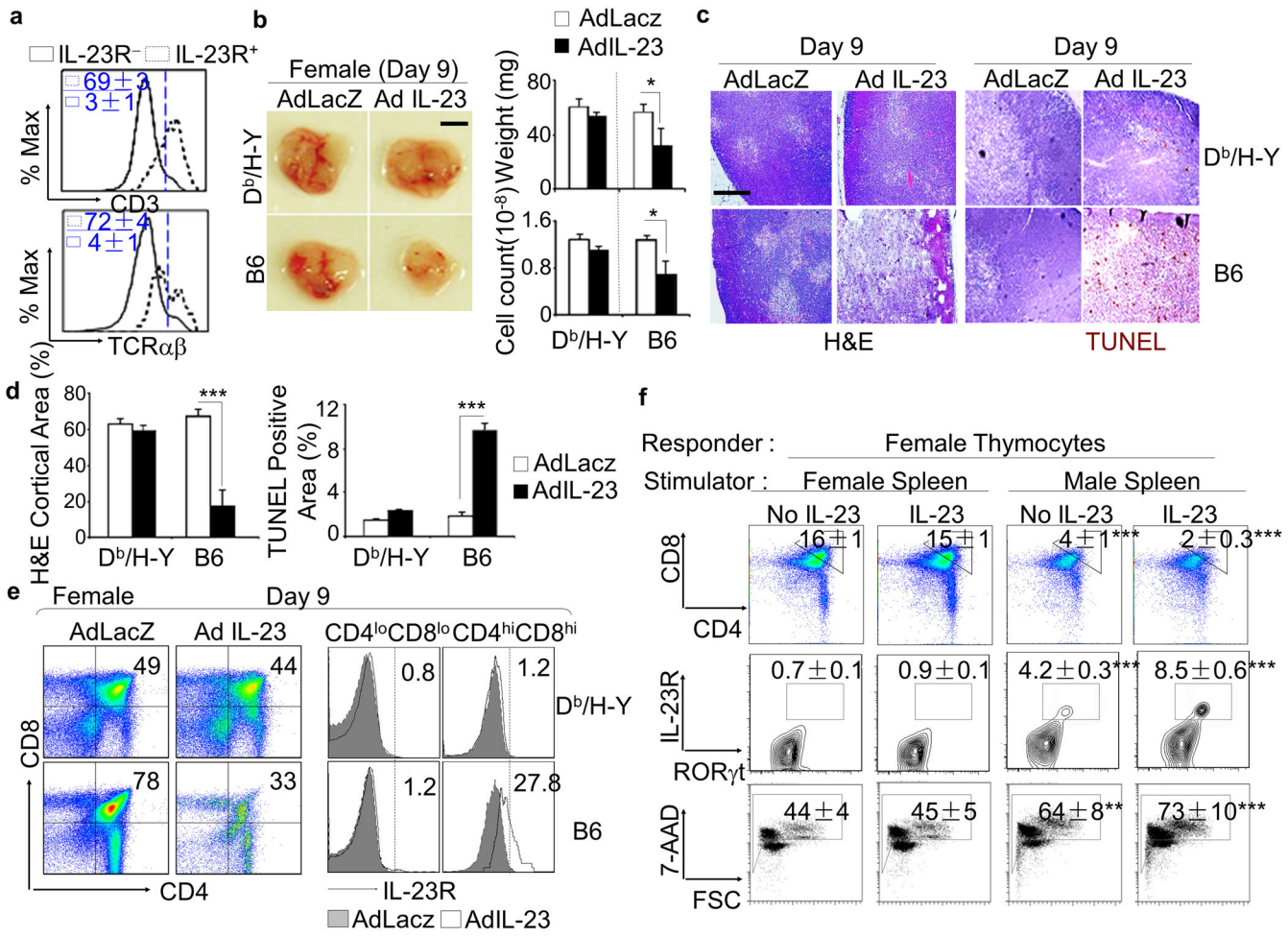

Figure 7. Antigen activation initiates the expression of IL-23R on CD4^{hi}CD8^{hi} DP thymocytes

(**a**) Flow cytometry analysis of the expression of αβTCR and CD3ε on IL-23R^{+}CD4^{+}CD8^{+} or IL-23R^{-} CD4^{+}CD8^{+} thymocytes from naïve C57L/B6J mice. The percentage of αβTCR^{+} or CD3ε^{+}cells in the indicated population is shown. (**b–e**) Female D^{b}/H-Y TCR Tg mice and female C57L/B6J mice were injected with either AdIL-23 or AdLacZ. Mice were sacrificed at day 9. (**b**) Left: Gross anatomic images showing the size of a representative thymus of the indicated mouse strains. Right: The weight and cellularity are shown. Scale bars: 3.0 mm. (**c**) *In situ* H&E (left) and *In situ* TUNEL staining (dark brown) (right) of a representative thymus section from the indicated group. The magnification of objective lens is 10x. Scale bars: 300 μm. (**d**) BioQuant quantitation of the frequency of thymic cortical area (left) or the frequency of TUNEL positive area (right) from ten randomly chosen areas. The results represent mean ± SEM (N=2–3 per group for 2 independent experiments, * p<0.05, ** p<0.01, *** p<0.005 for the indicated sample compared to AdLacZ injected group). (**e**) Left: Flow cytometry analysis of CD4 and CD8 expression on Thy1.2^{+} cells in the indicated group. The percent of CD4^{+}CD8^{+} cells is shown. Right: Flow cytometry analysis of IL-23R on CD4^{lo}CD8^{lo} and CD4^{hi}CD8^{hi} thymocytes. The percentage of IL-23R^{+} cells is indicated. (**f**) Thymocytes from female D^{b}/H-Y mice were cocultured *in vitro* with irradiated female or male splenocytes from Thy1.1 C57BL/6 in the presence or absence of exogenous mouse

recombinant IL-23. Top: Flow cytometry analysis of CD4 and CD8 expression on Thy1.2^{+} cells in the indicated group. The percent of CD4^{hi}CD8^{hi} cells is shown; Middle: The expression of IL-23R and RORγt on gated Thy1.2^{+}CD4^{+}CD8^{+} cells is shown; Bottom: Analysis of apoptosis (7-AAD) in Thy1.2^{+}CD4^{+}CD8^{+} cells. The percent of apoptotic cells is shown (N=3–4 mice per group for 2 independent experiments; * $p<0.05$, ** $p<0.01$, *** $p<0.005$ between thymocytes stimulated with female spleen cells in the absence of IL-23 compared to the indicated group).